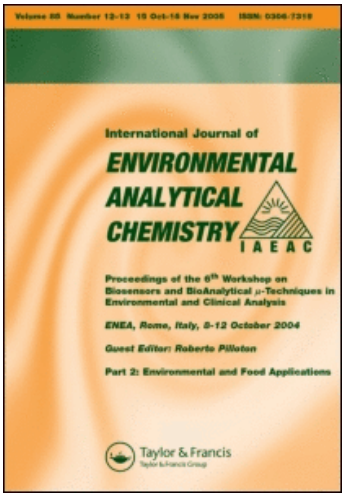

International Journal of Environmental Analytical Chemistry
Publication details, including instructions for authors and subscription information:
http://www.informaworld.com/smpp/title~content=t713640455

Determination of inorganic mercury using a polyaniline and polyaniline-methylene blue coated screen-printed carbon electrode

Vernon Somerset[a]; Joy Leaner[a]; Robert Mason[b]; Emmanuel Iwuoha[c]; Aoife Morrin[d]
[a] Water Ecosystems Research Group, NRE, CSIR, Stellenbosch, South Africa [b] Department of Marine Sciences, University of Connecticut, Groton, Connecticut, USA [c] SensorLab, Chemistry Department, University of the Western Cape, Bellville, South Africa [d] Sensors and Separations Group, Chemical Sciences Department, Dublin City University, Dublin 9, Ireland

Online publication date: 11 June 2010

To cite this Article Somerset, Vernon , Leaner, Joy , Mason, Robert , Iwuoha, Emmanuel and Morrin, Aoife(2010) 'Determination of inorganic mercury using a polyaniline and polyaniline-methylene blue coated screen-printed carbon electrode', International Journal of Environmental Analytical Chemistry, 90: 9, 671 — 685
To link to this Article: DOI: 10.1080/03067310902962536
URL: http://dx.doi.org/10.1080/03067310902962536

Intern. J. Environ. Anal. Chem.
Vol. 90, No. 9, 10 August 2010, 671–685

Taylor & Francis
Taylor & Francis Group

Determination of inorganic mercury using a polyaniline and polyaniline-methylene blue coated screen-printed carbon electrode

Vernon Somerset[a]*, Joy Leaner[a], Robert Mason[b], Emmanuel Iwuoha[c] and Aoife Morrin[d]

[a]*Water Ecosystems Research Group, NRE, CSIR, PO Box 320, Stellenbosch, 7599, South Africa;* [b]*Department of Marine Sciences, University of Connecticut, Groton, Connecticut, USA;* [c]*SensorLab, Chemistry Department, University of the Western Cape, Bellville, South Africa;* [d]*Sensors and Separations Group, Chemical Sciences Department, Dublin City University, Dublin 9, Ireland*

(*Received 17 November 2008; final version received 10 April 2009*)

Inorganic mercury ions (Hg^{2+}) in laboratory prepared solutions were determined with a screen-printed carbon electrode (SPCE) coated with a polyaniline-methylene blue (PANI-MB) polymer layer. The structure and properties of the PANI-MB polymer layer were compared to that of normal polyaniline (PANI) in order to elucidate the structure of the PANI-MB layer. The electrically-conducting polymers were prepared by electrochemical polymerisation of monomer solutions of aniline, and mixed solutions of aniline with methylene blue onto respective screen-printed carbon electrodes (SPCEs). Scanning Electron Microscopy (SEM) analyses of the SPCE polymer coated electrodes have shown that nanostructured materials have formed with the diameters of the PANI nanoclusters and PANI-MB nanorods at approximately 200 nm. Anodic stripping voltammetry (ASV) was used to evaluate a solution composed of 1×10^{-6} M Hg^{2+}, in the presence of the SPCE/PANI-MB polymer sensor electrode. The Hg^{2+} ions were determined as follows: (i) pre-concentration and reduction on the modified electrode surface and (ii) subsequent stripping from the electrode surface during the positive potential sweep. The experimental conditions optimised for Hg^{2+} determination included the supporting electrolyte concentration and the accumulation time. The results obtained have shown that the SPCE/PANI-MB polymer sensor electrode operates optimally at a pH 2, with the supporting electrolyte concentration at 0.5 M HCl. A linear calibration curve was found to be in the range of 1×10^{-8} M to 1×10^{-5} M Hg^{2+} after 120 s of pre-concentration. The detection limit was calculated and found to be 54.27 ± 3.28 μg L^{-1} of Hg^{2+}. The results have also shown that a conducting polymer modified SPCE sensor electrode can be used as an alternative transducer for the voltammetric stripping and analysis of inorganic Hg^{2+} ions.

Keywords: inorganic mercury determination; polyaniline nanoclusters; polyaniline-methylene blue nanorods; screen-printed carbon electrode (SPCE); differential pulse anodic stripping voltammetry (DPASV)

*Corresponding author. Email: vsomerset@csir.co.za

ISSN 0306–7319 print/ISSN 1029–0397 online

DOI: 10.1080/03067310902962536
http://www.informaworld.com

1. Introduction

Environmental pollution as a result of heavy metals is a worldwide problem. Traditional methods used to assess the magnitude of the environmental risk caused by heavy metal pollution, consists of sample digestion with strong acids, followed by chemical analysis and quantification of total metals. These techniques and methods are, however, unable to distinguish between potentially hazardous and non-hazardous fractions of metals, which often lead to damage to biological systems [1]. Apart from posing environmental risks, certain metals (e.g. calcium, cobalt, chromium, copper, iron, potassium, magnesium, manganese, sodium, nickel and zinc) are regarded as essential nutrients and play an integral role in the life processes of living organisms. In contrast, metals such as silver, aluminium, cadmium, gold, lead and mercury have no biological role and lead to toxicity when present. Metals (e.g. iron, copper) also serve as catalysts in biochemical reactions and may function as stabilisers of protein structures and bacterial cell walls, and also in maintaining osmotic balance.

Regardless of their status (i.e. essential or non-essential), if present in high concentrations, metals can be toxic for living cells, with mercury being one of the most toxic to living organisms [2]. Classical methods and techniques for determining mercury in the environment include atomic adsorption spectroscopy (AAS), atomic fluorescence spectroscopy (AFS), atomic emission spectroscopy (AES), inductively coupled plasma mass spectroscopy (ICP-MS), and capillary electrophoresis (CE). These are well established methods and are characterised by low detection limits (i.e. $0.02\,\mu g\,L^{-1}$ for AAS; $0.001\,ng\,L^{-1}$ for AFS; 0.01 for AES and 0.08 for ICP-MS). However, these classical techniques require expensive instrumentation and cannot be used for field and on-site measurements [2–8]. Alternatives to the classical methods and techniques include electrochemical methods of mercury determination (e.g. ion-selective electrodes (ISE); anodic stripping voltammetry (ASV); potentiometric stripping analysis (PSA); current stripping chronopotentiometry (CSP); and differential pulse voltammetry (DPV). However, these methods are characterised by high detection limits (i.e. $0.2\,ng\,L^{-1}$ for ASV; $0.5\,\mu g\,L^{-1}$ for PSA; $0.1\,\mu g\,L^{-1}$ for CSP and $2\,ng\,L^{-1}$ for DPV [2,9–13]. The analysis and detection of mercury in the environment is important, and the removal of mercury from effluent and waste streams has received much attention in this regard. To this end, several physical and chemical separation processes have been used that includes solvent extraction, ion-exchange processes, precipitation, membrane separation, reverse osmosis, coagulation, photo-reduction and complexation–ultrafiltration (CUF) [14–18].

The use of electrochemical sensors offers a novel approach towards measuring the bio-available mercury fraction in substrates, while both chemical sensors and biosensors provide a means of measuring mercury ions in aqueous solutions. Biosensors are able to combine a biological recognition element and a suitable transducer to perform analytical measurements. Various biosensor configurations have been developed that utilizes a variety of recognition elements, which include enzymes, whole cells, and various types of transducers. Meanwhile, several advances have also been made with the use of chemical sensors for the detection of heavy metal ions and pollutants in the environment [2,19–22].

The determination of Hg in the environment has become a priority due to the fact that Hg can bioaccummulate in the food chain and become a serious human health issue. Mercury exists in various chemical forms in nature with a wide range of physical, chemical and eco-toxicological properties that govern the environmental behaviour of each form. The three most important chemical forms of Hg known to be present in the environment

are: (i) elemental mercury (Hg^0) that has high vapour pressure and relatively low solubility in water; (ii) mercurous (Hg_2^{2+}) and mercuric (Hg^{2+}) inorganic cations that form the more soluble fraction and have a strong affinity for many inorganic and organic ligands, especially those containing sulphur; and (iii) organometallic compounds with one or two alkyl-/aryl- substituents, which are bound to the Hg atom, forming (mono-/di-) alkylated and/or arylated RHgX or RHgR′ (R = alkyl, R′ = aryl substituents) mercury species. Furthermore, the very water-soluble Hg^{2+} enters freshwater and marine resources by both wet and dry deposition, where it is rapidly converted into the more toxic methylmercury (CH_3Hg) form in the presence of sulphide reducing bacteria. This more toxic form bioaccumulates in the aquatic food chain and poses a serious health risk to humans who consume fish or other aquatic organisms that are contaminated with CH_3Hg.

Effective tools that will enable on-site analysis of trace metals in the field, has seen various developments and research activities explore the development of chemical sensors and biosensors. The main aim of the work presented here was to investigate the construction of chemical sensors that utilise specific polymers for inorganic mercury determination. In doing so, enhanced knowledge in the area of chemically modified electrodes for trace metal analysis will be generated.

The first objective was to optimise the conducting polymer parameters for the electrode preparation. Secondly, the possibility was explored of developing a stripping voltammetric assay for mercury ions (Hg^{2+}) in aqueous solutions using a disposable screen-printed carbon electrode. Voltammetry was used to investigate the electrochemical behaviour of Hg^{2+} in solution and to define the optimum instrumental conditions for the differential pulse anodic stripping voltammetric (DPASV) measurement of Hg^{2+} in aqueous solutions. Furthermore, the next stages of our future work will be to obtain new electrochemical sensors adapted to the determination of different species of mercury and other heavy metals applied to real samples, combining both, the incorporation of different and more selective receptor molecules at the SPCE surface and the selection of the adequate electrochemical reaction.

2. Experimental

2.1 *Materials and reagents*

The reagents aniline (99%) and *N*,*N*-dimethylformamide (98% atom D) were obtained from Aldrich, Germany. Potassium chloride, sulphuric acid (95%) and hydrochloric acid (32%) were purchased from Merck. Mercury(II) chloride (99.5%, ACS) and methylene blue (95%, extra pure) were purchased from Fluka (Germany) and used as received. All solutions were always prepared using ultra pure water obtained from a Milli-RO Milli-Q Plus (MilliporeWater) system.

2.2 *Instrumentation*

Electrochemical experiments were performed with a BioAnalytical Systems (BAS) 100B electrochemical analyser using cyclic voltammetry (CV), linear sweep stripping voltammetry (LSSV) or differential pulse anodic stripping voltammetry (DPASV) amperometric modes. A conventional three electrode system was employed consisting of a single

connector screen-printed working electrode, a BAS 3 M NaCl-type Ag/AgCl reference electrode, and a platinum wire auxiliary electrode. High purity argon gas was used to displace oxygen from the electrochemical cell before results were collected [23]. The screen-printed carbon electrodes (SPCEs) were obtained from the laboratories of the collaborators on this study, from the Sensors and Separations Group, Department of Chemical Sciences, Dublin City University, Dublin 9, Ireland. The fabrication of the SPCE is described in the papers of Morrin *et al.* [24] and Grennan *et al.* [25].

2.3 *Preparation of polyaniline-methylene blue (PANI-MB) polymer film*

Polyaniline (PANI) polymer films were prepared using a 10 mL solution consisting of 0.2 M aniline in aqueous 1 M HCl solution. Polyaniline (PANI) films were grown electrochemically on the surface of the screen-printed carbon electrode (SPCE) by repetitive cyclic voltammetry scanning at 100 mV/s from −200 to +1100 mV, for 10 cycles at 25°C.

For the PANI-MB film, a solution consisting of a 0.2 M aniline and 1 M HCl solution, as well as 0.002 M methylene blue (MB) solution was prepared. The PANI-MB polymer film was grown electrochemically on the surface of the SPCE by repetitive cyclic voltammetry scanning at 50 mV/s from −200 to +1100 mV, for 10 cycles. The SPCE was then rinsed with deionised water and immersed in fresh deionised water until use [25–27].

2.4 *Scanning electron miscroscopy (SEM) measurements*

SEM morphology studies were carried out on screen-printed carbon electrodes (SPCEs) coated with PANI and PANI-MB respectively, using a LEO 1525 Field Emission Scanning Electron Microscope (FE-SEM) with interchangeable accelerating voltages (maximum of 15.00 kV) for optimal sensitivity. Samples were mounted on aluminium stubs using conductive glue and were then coated with a thin layer of carbon [28–29].

2.5 *UV-Vis spectroscopic characterisation*

UV-Vis spectra were recorded between 200 and 1000 nm using a 1-cm path quartz cuvette and *N*,*N*-dimethylformamide (DMF) as the reference solvent, on a ThermoFisher Spectronic™ Helios™ range UV-Vis spectrometer with VISION PC software. Solutions for subsequent spectroscopic studies were obtained by collecting the different polymer layers, after electrodeposition on the SPCE surface and dissolving it from the electrode surface in DMF [30].

2.6 *FTIR spectroscopic characterisation*

The Fourier Transform Infrared (FTIR) spectra were recorded at wavenumber range of 400–4000 cm^{-1} for the polymer samples dissolved in DMF and recorded with a Bruker ALPHA-T, FT-IR spectrometer fitted with a Bruker Optics aligned RockSolid™ interferometer [28–29].

2.7 *Voltammetric electrode evaluation*

After preparation of the SPCE/PANI-MB (or SPCE/PANI) sensor electrode, the electrode was washed with copious amounts of deionised water and stored in 2 mL of deionised water at 4°C when not in use. For voltammetric evaluation, each of the SPCE/PANI and SPCE/PANI-MB sensor electrodes were immersed in a 2 mL solution of 1×10^{-6} M mercury chloride ($HgCl_2$). Laboratory solutions of different concentrations of $HgCl_2$ ranging from 1×10^{-5} M to 1×10^{-8} M were prepared using Milli-Q (Millipore) water and used in the electrode evaluation experiments. For all the experiments performed the pH of the solution was kept at approximately 1 with the use of 0.1 M H_2SO_4 as this pH is very suitable for inorganic mercury (Hg^{2+}) determination [31]. The effect of chloride ion concentration in Hg(II) determination was investigated and HCl concentrations of 0.0, 0.004, 0.005, 0.01, 0.05, 0.1 and 0.5 M were used as supporting electrolyte. No interferents were investigated at this stage of the study and its important contribution to the evaluation of the sensor will be investigated in future results.

All experiments were conducted using a three-electrode electrochemical cell containing Hg^{2+} and supporting electrolyte, described as (0.1 M H_2SO_4; 0.5 M HCl). DPASV was used to evaluate the electrochemical behaviour of the sensor electrode, while the results of the peak heights for the peak current (I_p) of the voltammograms were analysed [32]. Optimisation of the sensor electrode and the application of the SPCE/PANI-MB (or SPCE/PANI) sensor electrode was done in accordance with the methods developed by Faller *et al.* [31] and Crew *et al.* [33] for Hg^{2+} determination.

3. Results and discussion

3.1 *Polymerisation studies on SPCEs*

In the family of conducting polymers, polyaniline is a key material and has attracted intensive interest due to its promising electrical and electrochemical properties. Of the many applications of PANI reported over the years, its most promising application is in electrochemical sensing and biosensing [34]. In Figure 1(a) the cyclic voltammogram (CV)

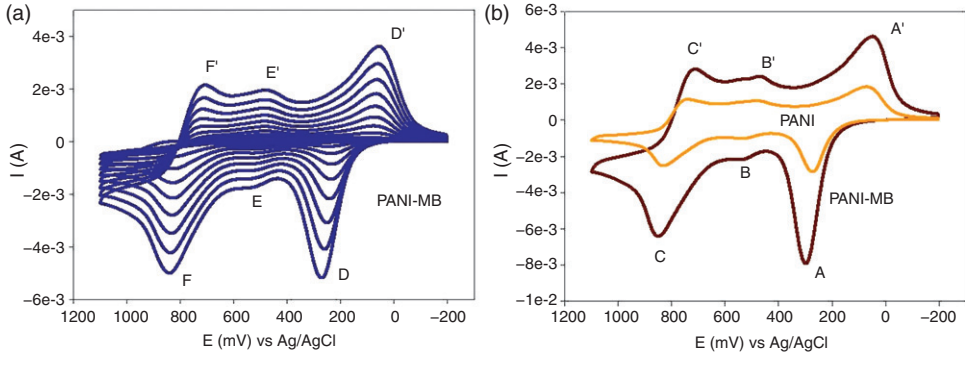

Figure 1. In (a) a cyclic voltammogram (CV) displaying the 10 cycles of electropolymerisation on a SPCE for PANI-MB is shown. The potential was cycled between −200 and +1100 mV at a scan rate of 100 mV/s. In (b) the CV displaying the 11th cycle of electropolymerisation on a SPCE for PANI and PANI-MB respectively is shown. The potential was cycled between −200 and +1100 mV at a scan rate of 50 mV/s for PANI-MB and 100 mV/s for PANI.

for the electropolymerisation of PANI-MB on a SPCE at a scan rate of 100 mV/s, in a potential window between −200 and +1100 mV is shown.

The results in Figure 1(a) illustrates that the PANI-MB polymer shows very good redox activity within the potential window at acidic pH. The CV obtained in Figure 1(a) also shows two main redox couples represented as (D/D′) and (F/F′) and the results are very similar as compared to PANI electropolymerisation on a platinum, gold or glassy carbon electrode [26,35,36]. Peaks D and F in the anodic scan corresponds to the transformation of leucoemeraldine base to emeraldine salt and the emeraldine salt to pernigraniline salt forms. For the cathodic scan, the main peaks D′ and F′ corresponds to the conversion of pernigraniline salt to emeraldine salt and emeraldine salt to leuco-emeraldine base. The small redox couple (E/E′) can be attributed to impurities such as benzoquinone and hydroquinone. Multiscan voltammetry resulted in an increase in the redox peaks which indicates the formation of a conducting polymer at the SPCE surface. The results further shows that the PANI electropolymerisation is the main driving force behind the conducting polymer electropolymerisation and coating on the SPCE surface as only the main peaks for this polymer are observed. Further structural, spectral and morphological results will show that the incorporation of MB in the polymer structure does occur [26,35,36].

In Scheme 1 the redox reaction of cationic methylene blue (MB^+) to leucomethylene blue at acidic pH is shown [37].

Results obtained by Karyakin *et al.* [38] for the electropolymerisation of MB on a gold disc electrode surface has shown that a growing polymer of poly(methylene blue) (PMB) was obtained when the potential was cycled between −400 to +1200 mV at a scan rate of 50 mV/s. In this electrosynthesis, a growing oxidation peak was observed at approximately + 180 mV (vs. Ag/AgCl) and a reduction peak at approximately −200 mV (vs. Ag/AgCl). These peaks seem to be completely masked by the first redox couple of PANI as represented by (D/D′) in Figure 1(a).

Analysis of the cyclic voltammograms (CVs) shown in Figure 1(b) indicates that an increase in peak current is observed for the PANI-MB polymer, as compared to the PANI polymer film. Both polymer films were electrosynthesised on SPCEs respectively and the 11th cycle of each polymer is shown in Figure 1(b). The enhanced redox character of the PANI-MB polymer film is clearly observed. The results obtained in this section for the PANI-MB polymer film will be further elucidated with structural, spectral and morphological results in the following paragraphs.

3.2 *Morphology*

The results obtained in the SEM micrographs shown in Figure 2 indicate that the morphology of the respective PANI (a) and PANI-MB (b) polymers is not only very well defined, but is also indicative of nanostructured material formation.

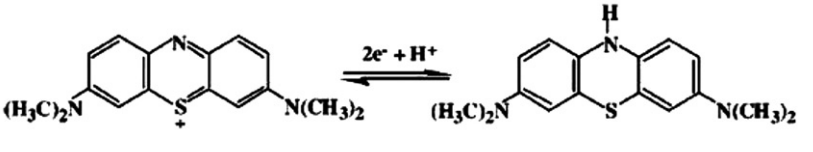

Scheme 1. Redox reaction of MB^+ to leucomethylene blue at acidic pH [36].

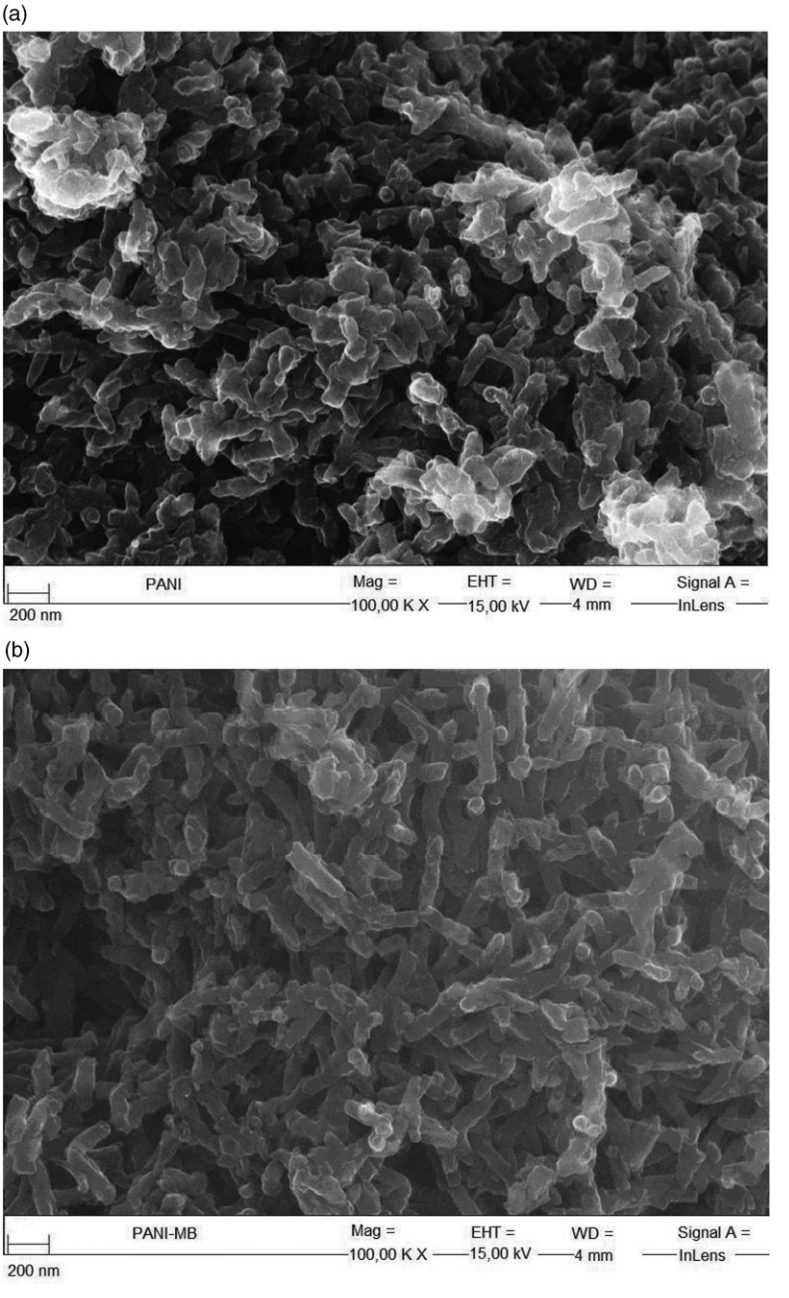

Figure 2. SEM micrographs of PANI nanoclusters in (a) and PANI-MB nanorods in (b), prepared at room temperature using 0.2 M aniline and 0.002 M methylene blue concentrations, respectively. Electropolymerisation was done on SPCE and the potential was cycled between −200 and +1100 mV at a scan rate of 100 mV/s for PANI and 50 mV/s for PANI-MB.

In Figure 2(a) the surface topography for PANI is shown with the formation of nanoclusters with a diameter of 200 nm visible, while more defined nanorods of diameter 200 nm in Figure 2(b) for PANI-MB was obtained. The experimental conditions of keeping the aniline concentration fixed at 0.2 M and optimising the MB concentration to 0.002 M, while performing the electropymerisation at a scan rate of 50 mV/s, are favourable for the shaping of uniform PANI-MB nanorods [28,39].

3.3 *UV-Vis absorption analysis*

The use of UV-Vis spectroscopy has been extensive as one of the convenient techniques in characterising the structures of intrinsically conductive polymers (ICPs) such as polyaniline (PANI). PANI is also known as one of the most studied ICPs and its UV-Vis spectrum is dominated by two absorption peaks at approximately 320 nm (band I) and 610 nm (band II). Band I at 320 nm can be assigned to the π–π^* transition and the nitrogen excitation in the benzenoid structure of PANI. Band II at 610 nm falls in the visible range of the electromagnetic spectrum and is ascribed to exciton formation in the quinonoid rings of PANI, giving rise to the green colour of PANI in dimethyl formamide (DMF) [30,40,41].

In Figure 3 the results for the UV-Vis spectroscopic analysis of the PANI and PANI-MB polymer films electropolymerised on the SPCE and dissolved in DMF solvent is shown. Analysis of the results in Figure 3 shows that for both PANI and the PANI-MB polymer films, absorption maxima at approximately 320 nm and 610 nm were observed to comply with the structural conformations highlighted in the above paragraph. In comparing the UV-Vis results of the PANI polymer film with that of the PANI-MB polymer film, it is seen that the band I results have a slightly lower peak height for the PANI-MB film. In comparing the band II results it is also observed that a small shift in the PANI-MB film maxima is observed that can be attributed to the structural differences of the PANI-MB film. The shift observed in band II at approximately 610 nm, indicates

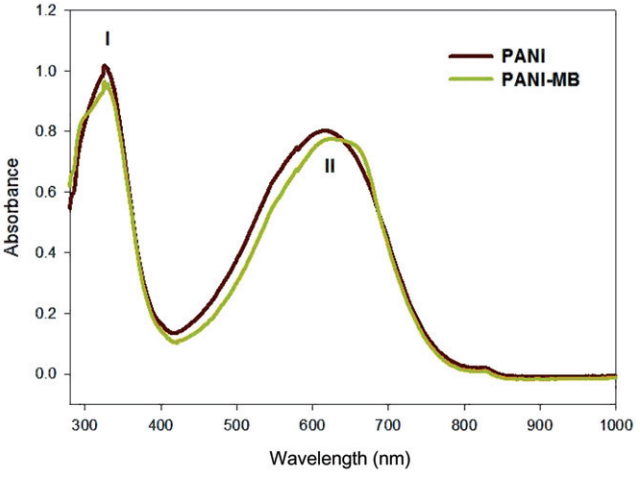

Figure 3. Results are shown for the UV-Vis spectra of PANI and PANI-MB polymer films obtained after electrochemical deposition on the SPCE surface followed by dissolution DMF solution.

that the maximum for polymer film PANI-MB occurs at a slightly longer wavelength, compared to the maximum observed for the PANI polymer film. This indicates that methylene blue (MB) had a bathochromic effect on the UV spectrum of PANI, indicating that substitution in the PANI structure has occurred.

In a study by Karyakin *et al*. [38] it was found that poly(methylene blue) (PMB) also exhibits 2 maxima in the UV-Vis analysis of the polymer film. The absorbance maxima can be observed at approximately 450 and 600 nm. The results in Figure 3 indicate that the two bands observed for PANI-MB at 320 and 610 nm are closely associated with the maxima of PMB and the observed results and the maxima for PANI-MB are attenuated by the stronger exciton formation in the quinonoid rings of PANI, giving rise to maxima II.

3.4 *FTIR spectral analysis*

Figure 4 represents the FTIR spectra of PANI and PANI-MB respectively, indicating the strong similarities and minute differences in structures.

The results in Figure 4 show that four and five characteristic stretching frequencies can be observed for the PANI and PANI-MB polymers, respectively. Band I at ca. 1250–1300 cm^{-1} are assigned to the C-N stretching in both polymer structures. Band II at ca. 1500–1600 cm^{-1} are assigned to the benzenoid aniline units of both polymers, while band III at ca. 1568–1587 cm^{-1} can be attributed to C=N quinoneimine stretching in both polymers. The weak stretching frequencies for band IV at ca. 3250–3500 cm^{-1} are due to the N-H absorption bands in the polymer structure, with the PANI-MB polymer having a fifth band at ca. 750 cm^{-1} for the C-S stretching assigned to the structure of MB [42,43].

3.5 *Optimisation of supporting electrolyte and deposition potential conditions*

Earlier research done by previous researchers has shown that a pH of 1 is very suitable for mercury (II) determination [31,44]. One of the experimental conditions optimised for the analysis of Hg(II) ions, was the chloride concentration of the supporting electrolyte.

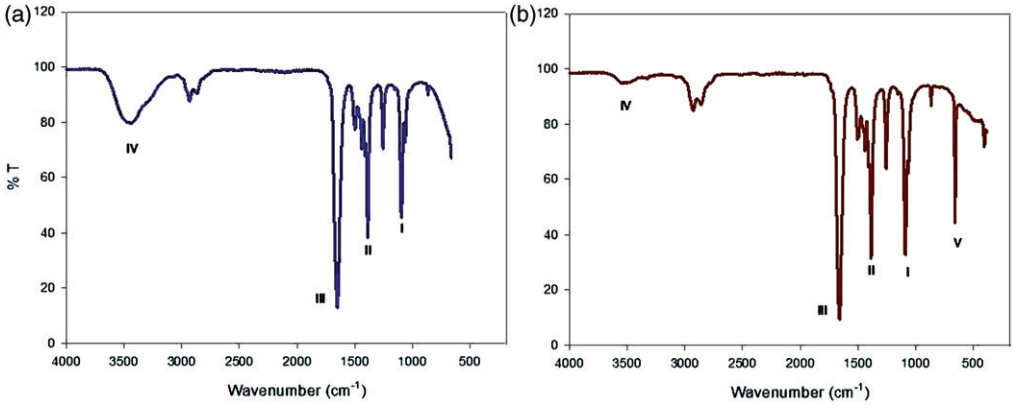

Figure 4. FTIR spectroscopy results with the spectra of PANI and PANI-MB polymer films obtained after electrochemical deposition on the SPCE surface followed by dissolution DMF solution.

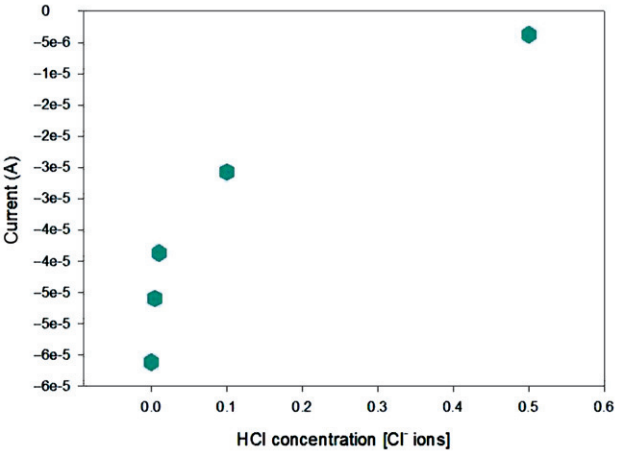

Figure 5. Results showing the effect of HCl supporting electrolyte concentration on the DPASV peak currents in a solution containing 0.1 M H_2SO_4 concentration; cHg(II) = 1×10^{-6} M, mercury concentration; and accumulation time (t_{acc}) of 120s; ($n = 3$).

As indicated in the experimental section, all the experiments were performed using a supporting electrolyte of 0.1 M H_2SO_4 [31].

Differential pulse anodic stripping voltammetry (DPASV) was used to collect current peak data ($I_{p,a}$) as it often offers better sensitivity and resolution than linear sweep voltammetry. In Figure 5 the DPASV data obtained for a solution containing 0.1 M H_2SO_4 concentration and mercury concentration [cHg(II)] of 1×10^{-6} M is shown, with the effect of varying hydrochloric acid (HCl) concentrations clearly indicated. In order to determine the optimum concentration of HCl to be added to the sample solution, a DPASV study was conducted using five different HCl concentrations. The results in Figure 5 shows a plot of the DPASV peak current versus the HCl concentration, showing that a 0.5 M HCl concentration would be appropriate for the proposed analysis. All experimental data were then collected using this HCl concentration [31,33].

In Figure 6(a), the results for the effect of the deposition potential (E_d) on the magnitude of the DPASV peak currents are shown.

The effect of the deposition potential (E_d) was studied using a solution containing 0.1 M H_2SO_4 concentration, 0.5 M HCl supporting electrolyte concentration and 1×10^{-6} M Hg^{2+} ion concentration. The results in Figure 6(a) shows the resulting peak currents ($I_{p,a}$) obtained for the Hg^{2+} ion stripping experiments, using a deposition time (t_{acc}) of 120 seconds. The magnitude of the peak obtained using different E_d values indicate that the largest value was obtained for an $E_d = -300$ mV, while the smallest value was obtained for $E_d = -400$ mV. No big differences in the $I_{p,a}$ values for the different deposition potentials were observed and the error was also relatively small for the three readings taken at each deposition potential.

The effect of deposition time on the magnitude of the DPASV currents obtained for each of the PANI and PANI-MB polymers in a solution containing 0.1 M H_2SO_4 concentration, 0.5 M HCl electrolyte concentration, and cHg(II) = 1×10^{-6} M, mercury concentration was also investigated. Different deposition times over the interval 0–300 seconds were investigated for the two different chemical sensors constructed. The aim of this experiment was to investigate the dependence between the mercury anodic peak data

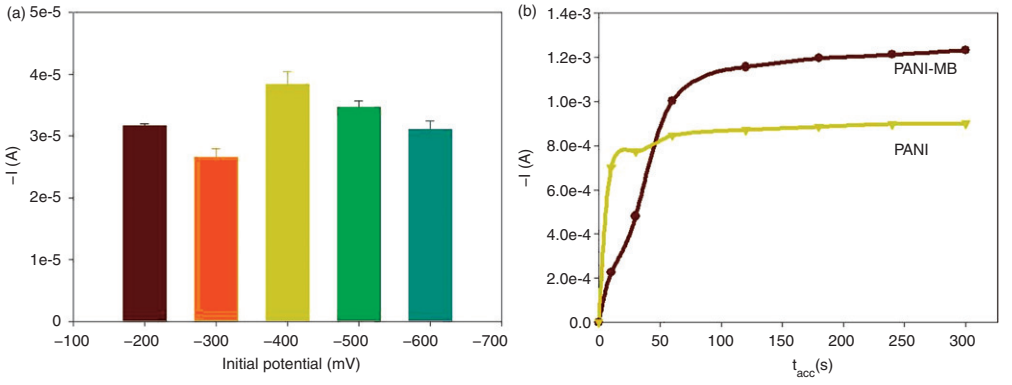

Figure 6. Results in (a) shows the effect of deposition potential on the DPASV peak currents in a solution containing 0.1 M H_2SO_4 concentration; 0.5 M HCl, electrolyte concentration; cHg(II) = 1×10^{-6} M, mercury concentration; and accumulation time (t_{acc}) of 120s; ($n = 3$). In (b) the results are shown for the effect of deposition time on the magnitude of the DPASV currents obtained for the PANI and PANI-MB polymers, respectively.

Table 1. Summary of optimum conditions for Hg^{2+} determination in aqueous samples.

	Determinant	Results
Reduction step	pH	1–2
	Reduction potential	−300 mV
	Reduction time	120s
	Supporting electrolyte	0.5 M HCl
Measurement step		
	Supporting electrolyte	0.5 M HCl
	Measurement technique	Differential pulse
	Potential window	−300 to +1500 mV

and the deposition time, over the interval 0–300 seconds. The results obtained for this investigation are shown in Figure 6(b). The results in Figure 6(b) indicate that the anodic peak current increases for deposition times of 0–120 s and thereafter remains relatively constant for the period up to 300 s evaluated. With the highest anodic peak currents obtained for the PANI-MB polymer film at approximately 120 s, we then decided to select a deposition time of 120 s for further studies.

Using the data collected in this study, the optimum conditions for Hg^{2+} determination in aqueous samples were identified and tabulated in Table 1. All subsequent differential pulse stripping voltammetry measurements were performed with the outlined steps.

3.6 *Sensor calibration and detection limit determination*

Calibration plots were constructed and evaluated under the chosen conditions summarised in Table 1. The calibration study was carried out using six different Hg^{2+} laboratory prepared standard solutions containing both 0.1 M H_2SO_4 and 0.5 M HCl acid concentrations. In Figure 7(a) a calibration plot for Hg^{2+} analysis using six different concentrations and its corresponding DPASV peak current data is shown.

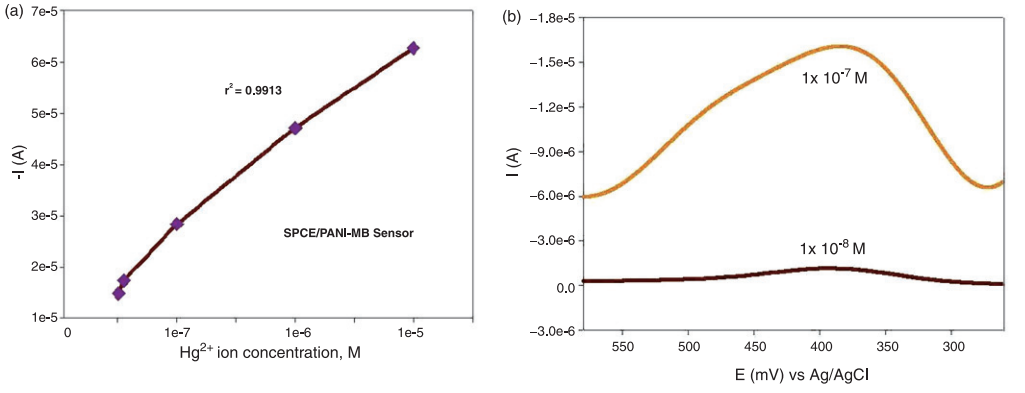

Figure 7. Results in (a) shows a calibration plot obtained for Hg^{2+} analysis in a solution containing 0.1 M H_2SO_4 concentration and 0.5 M HCl, electrolyte concentration using different DPASV peak current data, with a deposition potential (E_d) of −300 mV and deposition time (t_{acc}) of 120 s. The differential pulse anodic stripping voltammograms (DPASVs) in (b) were obtained for solutions containing different Hg^{2+} concentrations and 0.1 M H_2SO_4 concentration; 0.5 M HCl, electrolyte concentration; deposition potential (E_d) of −300 mV; and accumulation time (t_{acc}) of 120 s.

The results in Figure 7(a) were obtained by subjecting six different Hg^{2+} standards to DPASV analysis using the optimised E_d and t_{acc} values and a fresh SPCE/PANI + MB sensor for each measurement. The results in the graph indicate that the sensor exhibit a linear response between 1.0×10^{-6} and 5.0×10^{-6} M Hg^{2+} concentrations with a correlation coefficient of $r^2 = 0.9846$.

In Figure 7(b) the anodic peak potentials for two of the Hg^{2+} standards are shown, indicating that the peak potentials has shifted considerably for a small increase in the Hg^{2+} ion concentration. Similar trends were observed for the other Hg^{2+} standards applied in the sensor evaluation but are not shown here.

The SPCE/PANI+ MB sensor results were further evaluated to determine the limit of detection for the sensor. Using the results in Figure 7(a), the limit of detection (LOD) was calculated as the standard deviation multiplied by three and that value divided by the slope of the calibration plot in the linear range. The LOD value was found to be $54.27 \pm 3.28\ \mu g L^{-1}$ ($n = 10$). The LOD value for the SPCE/PANI+MB sensor compares favourably to the values obtained for other sensors constructed for the determination of Hg^{2+}. In the work done by Guo *et al.* [45], it was shown that a thin-film sol–gel-modified glassy carbon electrode functionalised with tetrasulfide has a detection limit of $100\ \mu g\ L^{-1}$. Similarly, Walcarius *et al.* [46] have shown that a carbon paste electrode modified with dispersed pure silica particles can detect Hg^{2+} at $10\ \mu g\ L^{-1}$. A very low detection limit of $1.4\ \mu g\ L^{-1}$ for Hg^{2+} determination was obtained by Zeij *et al.* [47], with the use of a carbon paste electrode containing sonogel and modified with poly(3-methylthiophene). The results of this study therefore demonstrate the possibility of applying a PANI-MB polymer film to the analysis of Hg^{2+} in aqueous solutions.

3.7 *Analysis of real samples*

The determination of inorganic mercury in two samples was performed to test the analytical procedure outlined in Table 1. Ultra pure water was spiked with $90\ \mu g\ L^{-1}$ of

Table 2. Determination of Hg^{2+} in real samples using SPCE/PANI+MB sensor.

Sample	Recovery (%)	Reference $[Hg^{2+}]$ ($\mu g\,L^{-1}$)	Detected $[Hg^{2+}]$ ($\mu g\,L^{-1}$)
SO1	92	90 (Added)	83 ± 4.3
SO2	95	120 (Added)	114 ± 3.1

Hg^{2+} to create sample SO1, while sample SO2 was created by spiking ultra pure water with $120\,\mu g\,L^{-1}$ of Hg^{2+}.

The results obtained for Hg^{2+} analysis in samples SO1 and SO2 with the SPCE/PANI+MB sensor is shown in Table 2. From the results in Table 2 it is seen that the proposed method was successfully applied to samples SO1 and SO2, indicating that the two samples spiked with known amounts of Hg^{2+} showed good recoveries (Table 2).

4. Conclusions

With the international call for a decrease in the use of Hg in all aspects of human activities in order to decrease mercury's impact on the environment and ecosystems, the use of Hg-free electrodes to perform stripping voltammetry is one step in that direction. We have investigated the redox characteristics of Hg^{2+} at SPCEs coated with a PANI-MB polymer film and found that well-defined oxidation peaks could be obtained in a solution containing 0.1 M H_2SO_4 concentration; 0.5 M HCl, electrolyte concentration and varying Hg^{2+} ion concentrations. SEM analyses of the SPCE polymer coated electrodes have shown that nanostructured materials were obtained. The developed SPCE/PANI + MB sensors present the advantages of small size, simple fabrication methods and handling, and reusability. The results obtained with the sensor has also shown that using an easy and low-cost methodology, satisfactory experimental results could be obtained for Hg^{2+} ion determination in aqueous solutions. The results further indicate that the analytical methodology developed showed adequate response times with a deposition time of 120 s required in the determination of Hg^{2+} ions in the samples evaluated. Lastly, it was found that the sensor has a detection limit of $54.27 \pm 3.28\,\mu g\,L^{-1}$ that is well within the range of other SPCE sensors quoted in literature.

Acknowledgements

This research was supported by funding received from the CSIR's parliamentary grant (PG) process and the National Research Foundation (NRF) of South Africa in aide of the South African Mercury Assessment Programme's (SAMA) research activities into the quantification of Hg levels in South African water resources. The collaboration with the research laboratories of the Universities of the Western Cape (RSA), Dublin City University (DCU) and Connecticut (USA) is also acknowledged.

References

[1] A. Ivaska, M. Virta, and A. Kahrua, Soil Biol. Biochem. **34**, 1439 (2002).
[2] I. Bontidean, A. Mortari, S. Leth, N.L. Brown, U. Karlson, M.M. Larsen, J. Vangronsveld, P. Corbisier, and E. Csoregi, Environ. Poll. **131**, 255 (2004).

[3] H. Emteborg, H.W. Sinemus, B. Radziuk, D.C. Baxter, and W. Frech, Spectrochim. Acta B **51**, 829 (1996).
[4] D. Cossa, J. Sanjuan, J. Cloud, P.B. Stockwell, and W.T. Corns, J. Anal. Atom. Spectr. **10**, 287 (1995).
[5] B. Jamoussi, M. Zafaouf, and B. BenHassine, Intl. J. Environ. Anal. Chem. **61**, 249 (1995).
[6] H. Hintelmann, R.D. Evans, and J.V. Villeneuve, J. Anal. Atom. Spectros. **10**, 619 (1995).
[7] Z.-L. Peng, F. Qu, Q. Song, and J.-M. Lin, Electrophor. **26**, 3333 (2005).
[8] W. Liu and H.K. Lee, J. Chroma. A **796**, 385 (1998).
[9] J.A. Shatkin, H.S. Brown, and S. Licht, Anal. Chem. **67**, 1147 (1995).
[10] J. Wang and B. Tian, Anal. Chim. Acta **274**, 1 (1993).
[11] E. Beinrohr, M. Cakrt, J. Dzurov, P. Kottas, and E. Kozakova, Fresenius J. Anal. Chem. **365**, 253 (1996).
[12] P. Ugo, L.M. Moretto, and G.A. Mazzocchin, Anal. Chim. Acta **305**, 74 (1995).
[13] L.S. Dolci, E. Marzocchi, M. Montalti, L. Prodi, D. Monti, D. Di Natale, C. D'Amico, and R. Paolesse, Biosens. Bioelectron. **22**, 399 (2006).
[14] F.-S. Zhang, J.-O. Nriagu, and H. Itoh, Water Res. **39**, 389 (2005).
[15] S. Chiarle, M. Ratto, and M. Rovatti, Water Res. **34**, 2971 (2000).
[16] K. Larson, Ind. Eng. Chem. Res. **31**, 2714 (1992).
[17] L.R. Skubal and N.K. Meshkov, J. Photochem. Photobiol. A: Chem. **148**, 211 (2002).
[18] J. Barron-Zambrano, S. Laborie, P. Viers, M. Rakib, and G. Durand, J. Membrane Sci. **229**, 179 (2004).
[19] A. Amine, C. Cremisini, and G. Palleschi, Mikrochim. Acta **121**, 183 (1995).
[20] L.D. Rasmussen, S.J. Sørensen, R.R. Turner, and T. Barkay, Soil Biol. Biochem. **32**, 639 (2000).
[21] I. Bontidean, W. Schuhmann, and E. Csoregi, in *Biosensors for monitoring of metal ions*, edited by R. Cornelis, Handbook of Elemental Speciation (Wiley & Sons, Chichester, UK, 2003).
[22] I. Palchetti, S. Laschi, and M. Mascini, Anal. Chim. Acta **530**, 61 (2005).
[23] V.S. Somerset, M.J. Klink, M.M.C. Sekota, P.G.L. Baker, and E.I. Iwuoha, Anal. Lett. **39**, 1683 (2006).
[24] A. Morrin, O. Ngamna, E. O'Malley, N. Kent, S.E. Moulton, G.G. Wallace, M.R. Smyth, and A.J. Killard, Electrochim. Acta **53**, 5092 (2008).
[25] K. Grennan, A.J. Killard, and M.R. Smyth, Electroanal. **13**, 745 (2001).
[26] V.S. Somerset, M.J. Klink, P.G.L. Baker, and E.I. Iwuoha, J. Envir. Sci. Health B **42**, 297 (2007).
[27] X. Li, M. Zhong, C. Sun, and Y. Luo, Mat. Lett. **59**, 3913 (2005).
[28] R. Akinyeye, I. Michira, M. Sekota, A. Al-Ahmed, P. Baker, and E. Iwuoha, Electroanal. **18**, 2441 (2006).
[29] V.S. Somerset, L.F. Petrik, R.A. White, M.J. Klink, D. Key, and E. Iwuoha, Talanta **64**, 109 (2004).
[30] Y. Wang and X. Jing, Polym. Testing **24**, 153 (2005).
[31] C. Faller, N.Y. Stojko, G. Henze, and K.Z. Brainina, Anal. Chim. Acta **396**, 195 (1999).
[32] G. Cabello-Carramolino and M.D. Petit-Dominguez, Anal. Chim. Acta **64**, 103 (2008).
[33] A. Crew, D.C. Cowell, and J.P. Hart, Talanta **75**, 1221 (2008).
[34] X. Luo, A.J. Killard, A. Morrin, and M.R. Smyth, Electrochim. Acta **52**, 1865 (2007).
[35] A. Morrin, O. Ngamna, A.J. Killard, S.E. Moulton, M.R. Smyth, and G.G. Wallace, Electroanal. **17**, 423 (2005).
[36] E.I. Iwuoha, D. Saenz de Villaverde, N.P. Garcia, M.R. Smyth, and J.M. Pingarron, Biosens. Bioelectron. **12**, 749 (1997).
[37] T. Komura, G.Y. Niu, T. Yamaguchi, M. Asano, and A. Matsuda, Electroanal. **16**, 1791 (2004).
[38] A. Karyakin, E.E. Karyakina, and H.-L. Schmidt, Electroanal. **11**, 149 (1999).
[39] N.G.R. Mathebe, A. Morrin, and E.I. Iwuoha, Talanta **64**, 115 (2004).
[40] N. Kohut-Svelko, S. Reynaud, and J. Francois, Synth. Metals **150**, 107 (2005).
[41] W. Dhaoui, H. Zarrouk, and A. Pron, Synth. Metals **157**, 564 (2007).

[42] S. Bhadra, N.K. Singha, and D. Khastgir, J. Appl. Polymer Sci. **104**, 1900 (2007).
[43] T.-C. Wen, L.-M. Huang, and A. Gopalan, Synth. Metals **12**, 451 (2001).
[44] W. Huang, C. Yang, and S. Zhang, Anal. Bioanal. Chem. **374**, 998 (2002).
[45] Y. Guo and A.R. Guadalupe, J. Pharm. Biomed. Anal. **19**, 1221 (2008).
[46] A. Walcarius, J. Devoy, and J. Bessiere, J. Solid State Electrochem. **6**, 330 (2000).
[47] H. Zeij, P. Sharrock, J.L. Hidalgo Hidalgo-de Cisneros, I. Naranjo-Rodriguez, and K.R. Temsamani, Talanta **68**, 79 (2005).